Surgery 165 (2019) 114–123

Contents lists available at ScienceDirect

Surgery

journal homepage: www.elsevier.com/locate/surg

Innovative surgical guidance for label-free real-time parathyroid identification ☆

Giju Thomas, PhD[a,b], Melanie A. McWade, PhD[a,b], John Q. Nguyen, PhD[a,b], Melinda E. Sanders, MD[c], James T. Broome, MD[d], Naira Baregamian, MD[e], Carmen C. Solórzano, MD[e], Anita Mahadevan-Jansen, PhD[a,b,*]

[a] Vanderbilt Biophotonics Center, Vanderbilt University, Nashville, TN
[b] Department of Biomedical Engineering, Vanderbilt University, Nashville, TN
[c] Department of Pathology, Microbiology and Immunology, Vanderbilt University, Nashville, TN
[d] St. Thomas Medical Partners – Endocrine Surgical Specialists, Nashville, TN
[e] Division of Surgical Oncology and Endocrine Surgery, Vanderbilt University, Nashville, TN

ARTICLE INFO

Article history:
Accepted 3 April 2018
Available online 12 November 2018

ABSTRACT

Background: Difficulty in identifying the parathyroid gland during neck operations can lead to accidental parathyroid gland excisions and postsurgical hypocalcemia. A clinical prototype called as PTeye was developed to guide parathyroid gland identification using a fiber-optic probe that detects near-infrared autofluorescence from parathyroid glands as operating room lights remain on. An Overlay Tissue Imaging System was designed concurrently to detect near-infrared autofluorescence and project visible light precisely onto parathyroid gland location.

Methods: The PTeye and the Overlay Tissue Imaging System were tested in 20 and 15 patients, respectively, and a modified near-infrared imaging system was investigated in 6 patients. All 41 patients underwent thyroidectomy or parathyroidectomy. System accuracy was ascertained with surgeon's visual confirmation for in situ parathyroid glands and histology for excised parathyroid glands.

Results: There was no observable difference between near-infrared autofluorescence of healthy and diseased parathyroid glands. The PTeye identified 98% of the parathyroid gland, whereas the near-infrared imaging system and the Overlay Tissue Imaging System identified 100% and 97% of the parathyroid glands, respectively.

Conclusion: The PTeye can guide in real-time parathyroid gland identification even with ambient operating room lights. The near-infrared imaging system performs parathyroid gland imaging with high sensitivity, whereas the Overlay Tissue Imaging System enhances parathyroid gland visualization directly within the surgical field without requiring display monitors. These label-free technologies can be valuable adjuncts for identifying parathyroid glands intraoperatively.

Introduction

Accidental excision or damage to a healthy parathyroid gland (PG) during thyroidectomy and the inability to identify diseased PGs during parathyroidectomy can result in postsurgical complications. Incidental PG removal occurs in 5%–22% of the thyroid operations,[1] causing transient hypocalcemia (<6 months) in 15%–30% of cases or permanent hypocalcemia (>6 months) in up to 7% of the patients.[2] In comparison, failure to identify and remove diseased PGs occurs in 5%–10% of parathyroidectomies and can lead to persistent hyperparathyroidism,[3] necessitating a repeat operation that is associated with greater rates of complication and costs.[4,5] Although preoperative imaging modalities, such as ultrasonography imaging, Technetium-99m sestamibi scintigraphy, and computed tomography (CT), can aid in localizing diseased PGs with varying success,[6] many surgeons still identify PGs intraoperatively using visual examination where the accuracy can vary depending on experience.[7,8] PG tissue is ultimately confirmed by frozen section analysis and indirectly by intraoperative parathyroid hormone assays that are invasive, require repeat sampling, and need a wait time of 20–30 minutes per sample.[9,10] Therefore a noninvasive, label-free,

☆ Presented at the 39th annual meeting of the American Association of Endocrine Surgeons in Durham, North Carolina, May 6–8, 2018.

* Corresponding author: Professor Anita Mahadevan-Jansen, PhD, Vanderbilt Biophotonics Center, Department of Biomedical Engineering, Vanderbilt University, Station B, Box 351631, Nashville, Tennessee 37325.
E-mail address: anita.mahadevan-jansen@vanderbilt.edu (A. Mahadevan-Jansen).

https://doi.org/10.1016/j.surg.2018.04.079
0039-6060/

rapid, highly accurate intraoperative tool would be very valuable in identifying PGs.

Paras et al was the first to demonstrate noninvasive and label-free PG identification regardless of disease state using near-infrared autofluorescence (NIRAF) detection. This finding was subsequently validated with high accuracy by McWade et al.[11,12] The phenomena is based on the fact that PGs emit a stronger NIRAF signal compared with adjacent neck tissues, which has been investigated with promising results by several other groups.[13–16] Among the various systems that have been explored for NIRAF-based PG identification, the spectroscopy-based systems with handheld fiber-optic probes present tissue NIRAF as spectral data, whereas near-infrared (NIR) imaging systems depict grayscale images on remote display monitors. Despite high accuracy in PG identification, both these modalities present data in a format not easily utilized by surgeons. Although NIR imaging systems provide valuable spatial information about the PG, the images may be subject to erroneous interpretations because alignment of anatomic structures observed in NIR images may not be easily translated easily to what is visualized directly in the operative field.[17,18] Both these modalities are also prone to interference from NIR components in operating room (OR) lights during tissue NIRAF detection, requiring OR lights to be switched off frequently causing surgical workflow interruption.

To address the described challenges, we optimized our previous fiber-based spectroscopy system[11,12] and developed a handheld surgical guidance device called the PTeye abbreviated for the parathyroid eye (AiBiomed Inc, Santa Barbara, CA, and Vanderbilt University, Nashville, TN) that can optimally function with ambient OR lights and has a distinct user-interface that can be interpreted more easily by surgeons. In parallel, we developed an Overlay Tissue Imaging System (OTIS) that collects tissue NIRAF signal and projects it as a visible image directly onto the operative field, thus minimizing the need for remote display monitors and incorrect image interpretations.

In this study, we sought to evaluate the performance of these 2 novel devices in accurately identifying or visualizing PGs in comparison with a modified commercial NIR imaging system. Because most available NIR imaging systems are designed primarily for detecting NIR fluorescence from contrast agents, such as indocyanine green, this system was modified for label-free PG visualization as described earlier.[19] This study eventually aims to showcase the various technologic innovations that could ensure rapid, noninvasive, label-free intraoperative PG identification with minimal workflow disruption, while assessing merits and limitations for all the 3 devices.

Methods

Patient selection

Patients (18–99 years of age) who presented at the Vanderbilt Endocrine Surgery Center for thyroidectomy or parathyroidectomy were recruited based on the eligibility as assessed by the respective surgeon during preoperative assessment. Informed written consent was obtained from all patients recruited for this study, which was approved by the Institutional Review Board of Vanderbilt University. A total of 41 patients were recruited: 20 for the PTeye, 6 for the modified NIR imaging system, and 15 for the OTIS. Patient data were acquired and stored in compliance with the HIPAA privacy rule.

NIRAF detection with the PTeye

The PTeye (Fig. 1) comprises a console encasing a 785 nm laser source and a detector, a detachable and sterilizable fiber-optic probe, a foot pedal to activate NIRAF measurements, and a display panel. The PTeye probe delivers laser light at a power of 20 mW over a spot size of ~400 μm. Although it is based on the earlier system,[11,12] the internal circuitry of the PTeye is designed to detect NIRAF without interference from ambient OR lights. Tissue NIRAF recorded with PTeye is conveyed to the display panel and to the loudspeaker as auditory feedback. The display panel informs the surgeon on the "detection level" (absolute tissue NIRAF intensity), the "detection ratio" (tissue NIRAF normalized to the thyroid NIRAF intensity), and the "detection percentage" (the PTeye confidence in identifying PGs [calibrated to the "detection ratio"]). The auditory feedback commences once the "detection ratio" reaches a threshold value set for PG identification.[11,12]

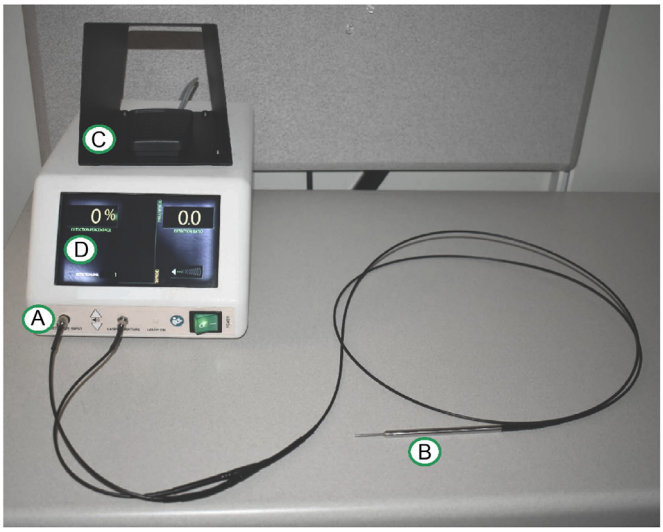

Fig. 1. The parathyroid eye (PTeye) system. (*A*) The console that encloses the laser and detector, (*B*) a detachable and sterilizable fiber-optic probe, (*C*) a foot-pedal that activates tissue near-infrared autofluorescence (NIRAF) detection, and (*D*) a display that intuitively informs the surgeon if the tissue is parathyroid or not.

The surgeon first confers the degree of confidence in having identified PG tissue as high, moderate, or low, based on visual inspection of the tissue in view. The surgeon then places the handheld probe of the PTeye on the tissue site and presses the foot pedal, after which tissue NIRAF intensity is displayed in real time with the OR lights remaining on. In each patient, a NIRAF baseline was first established on the thyroid so that subsequent tissue NIRAF measurements in the patient could be normalized to this thyroid baseline for obtaining the "detection ratio" described earlier. The auditory feedback volume was kept inaudible and the PTeye display panel was turned away to decrease bias of the surgeon's judgment.

NIRAF imaging with the modified commercial NIR imaging system

The commercial NIR imaging system is composed of a 3-chip, color camera with an integrated zoom lens (Karl Storz, PDD Camera El Segundo, CA) driven by a control unit (Karl Storz, Tricam SL, El Segundo, CA).[19] The system has a spatial resolution of 170 μm on a surgical field measuring 5 cm × 5 cm, and the 785 nm laser evenly illuminated the operative field at 1 W/cm^2. This commercial NIR system was modified to block the 785 nm laser beam used while allowing white light and NIRAF image capture (Fig. 2). On finding a parathyroid candidate, the surgeon degree of confidence was first recorded, after which NIRAF images were acquired with the OR lights turned off.

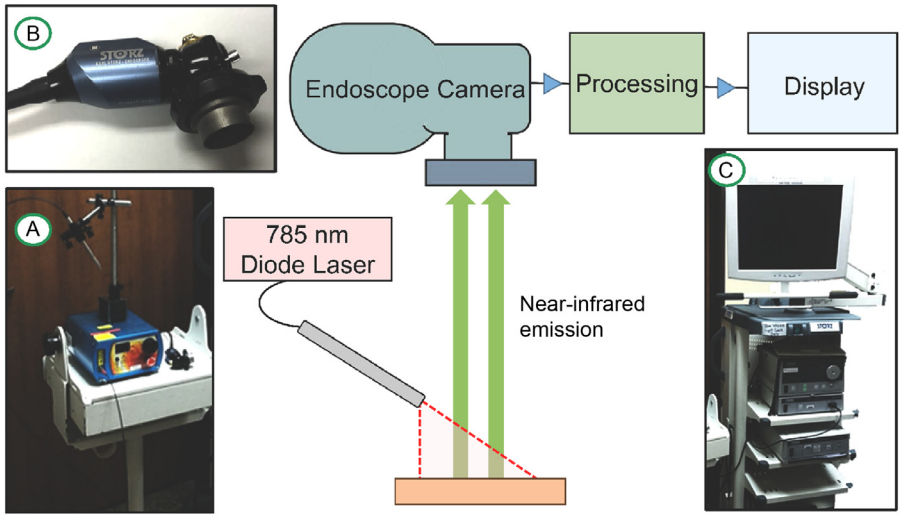

Fig. 2. A modified commercial near-infrared (NIR) imaging system comprises (*A*) a 785 nm laser source (for tissue illumination); (*B*) a commercial NIR camera (Karl Storz) that has been modified to permit near-infrared autofluorescence (NIRAF) and white light capture of the operative field, and (*C*) a control unit with a remote display monitor to visualize the acquired NIRAF images.

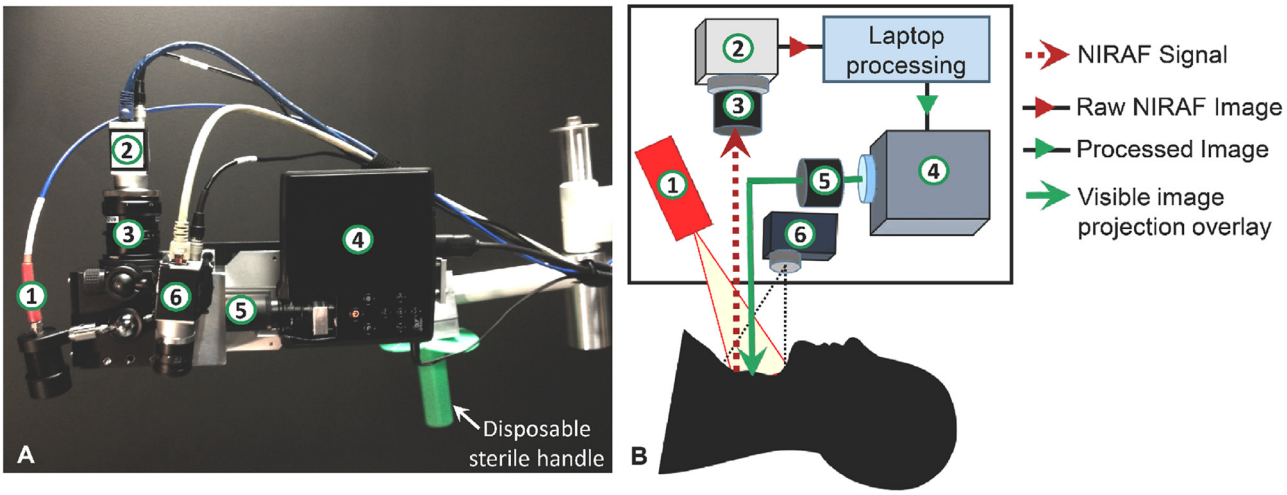

Fig. 3. (*A*) Components of the Overlay Tissue Imaging System (OTIS) are as follows: (1) a 785 nm laser source output, (2) a near infrared (NIR) camera, (3) coupling optics, (4) a visible image projector, (5) focusing optics for outgoing projection signal, and (6) a color camera to image the operative field; *B*. Workflow in the OTIS–NIRAF (near-infrared autofluorescence) detection from tissue followed by visible image projection overlay directly onto the tissue within the operative field.

Parathyroid visualization with the OTIS

The OTIS, seen in Fig. 3, *A*, was custom-built and consisted of a 785 nm diode laser (Innovative Photonics Solutions, Monmouth Junction, NJ), a NIRAF image collection unit, coupling optics, a visible light projector, focusing optics, and an image processing laptop. The NIRAF image collection unit includes a filtered NIR camera (Basler AG, Ahrensburg, Germany). At a distance of 50 cm from a operative field measuring 5 cm × 6.25 cm, the OTIS has a spatial resolution of 176 µm. When the operative field is diffusely illuminated with the 785 nm laser at an irradiance of 11.5 mW/cm^2, tissue NIRAF signal is picked by the NIR camera through the coupling optics, as seen in Fig. 3, *B*. Raw NIR images are then relayed to the image processing laptop and subsequently transmitted to a visible light projector (AAXA Technologies, Irvine, CA) which overlays a visible image through focusing optics precisely onto the operative field. An additional color camera (Basler AG, Ahrensburg, Germany) is integrated to record the projected overlay images. The components of OTIS are fixed onto a surgical support arm that can be positioned at any required angle by the surgeon using a disposable sterile handle (Fig. 3, *A*).

Before each patient testing, spatial precision of the OTIS projected image was assessed using a grid sketched with fluorescent ink and calibrated accordingly. Once a parathyroid candidate was seen, the surgeon confidence level in visually identifying each parathyroid gland was noted. The OTIS was then positioned by the surgeon above the region of interest with the help of a projected visible white rectangle. After the OR lights were turned off, NIRAF signals were collected, processed, and projected directly as visible green images onto the surgical site. The surgeon looked away during the OTIS projection to keep surgical decision-making unbiased.

Data analysis

NIRAF intensity was normalized to the thyroid NIRAF baseline to generate “detection ratio” for the PTeye, whereas NIRAF intensity obtained with the NIR imaging system and the OTIS was standardized to that of the adjacent tissue (background) to obtain

Table 1
Demographics of patients evaluated with the NIRAF based guidance modalities for parathyroid identification.

Patient Demographic variables	PTeye	(Modified) NIR imaging system	OTIS
Total number of patients	20	6	15
Age (in years)			
Mean ± Standard Deviation *(Range)*	46.8 ± 14.2 *(21–70)*	54.8 ± 17.6 *(29–75)*	55.1 ± 13.1 *(29–70)*
Gender			
Male	4 (20.0%)	3 (50.0%)	4 (26.7%)
Female	16 (80.0%)	3 (50.0%)	12 (73.3%)
Ethnicity			
Caucasian	17 (85.0%)	5 (83.3%)	14 (93.3%)
Non-Caucasian	3 (15.0%)	1 (16.7%)	1 (6.7%)
Body Mass Index (in kg/m^2)			
Mean ± Standard Deviation *(Range)*	30.6 ± 7.9 *(24.2–50.2)*	26.5 ± 6.9 *(16.4–33.1)*	28.9 ± 6.6 *(20.5–47.8)*
Disease type			
Benign thyroid disease	8 (40.0%)	2 (33.3%)	3 (20.0%)
Malignant thyroid disease	1 (5.0%)	1 (16.7%)	5 (33.2%)
Graves' Disease	1 (5.0%)	0 (0.0%)	1 (6.7%)
Primary Hyperparathyroidism			
Solitary adenomas	5 (25.0%)	2 (33.3%)	3 (20%)
Multiglandular disease	3 (15.0%)	0 (0.0%)	1 (6.7%)
Secondary hyperparathyroidism	0 (0.0%)	0 (0.0%)	1 (6.7%)
Concurrent thyroid and parathyroid disease			
Primary Hyperparathyroidism	1 (5.0%)*	1 (16.7%)†	1 (6.7%)
Secondary hyperparathyroidism	1 (5.0%)*	0 (0.0%)	0 (0.0%)

* associated with malignant thyroid disease
† associated with benign thyroid disease

the NIRAF ratios. A 2-tailed Student *t*-test was used to compare measured ratios of parathyroid and nonparathyroid tissues with values of $P < .05$ being considered statistically significant. Detection rate for each system was determined by correlating the number of tissues deemed PG positive by the system (Threshold: Detection or NIRAF ratio >1.2) with the number of PG tissues confirmed using histology for excised or biopsied PGs, or visual inspection by participant surgeons.

Results

Table 1 summarizes the demographics of the 41 patients recruited for this study. Measurements were obtained using the PTeye on 55 PGs (107 sites) and 198 nonparathyroid tissues (ie, thyroid, fat, lymph node, muscle, and trachea) in 20 patients. The modified NIR imaging system was tested over 9 PGs in 6 patients, and the OTIS was evaluated across 35 PGs in 15 patients.

The handheld probe of the PTeye was utilized as seen in Fig. 4, *A* in the presence of ambient OR lights to first establish a thyroid NIRAF baseline (Fig. 4, *B*) and obtain subsequent tissue measurements. Examples of "positive" and "negative" measurements for PG as indicated on the PTeye display are represented in Fig. 4, *C* and 4, *D*, respectively. The averaged detection ratio measured with PTeye in PGs was 3.7 (95% Confidence interval: 3.4–4.1) when compared to the averaged detection ratio of non-parathyroid tissues (i.e. thyroid, fat, muscle, lymph node and trachea) which was 0.7 (95% Confidence interval: 0.6–0.8). Averaged detection ratio of healthy PGs ($n = 33$) was measured to be 3.7 (95% Confidence interval: 3.3–4.1) and that of diseased PGs ($n = 22$) was found to be 3.7 (95% Confidence interval: 3.2–4.3). Based on these ratios, the PTeye yielded a 97% sensitivity (104/107 parathyroid measurements) and 95% specificity (188/198 nonparathyroid measurements). The surgeons found 50 PGs (detection rate: 91%) with high or moderate confidence, using simple visual examination by relying on their individual experience. In comparison, the PTeye identified 54 of 55 PGs with a 98% detection rate.

The modified NIR imaging system was investigated for PG identification as illustrated in Fig. 5, *A* with the OR lights off. The operative field with the PG as visualized with the naked eye is represented in Fig. 5, *B,* and the corresponding NIRAF image as displayed on the system monitor can be seen in Fig. 5, *C*. PGs exhibited NIRAF ratios that were approximately 2.1 times greater than those of the nonparathyroid background. Averaged NIRAF ratios of healthy PGs measured 2.2 (95% Confidence interval: 2.0–2.4), whereas the diseased PGs ($n = 3$) recorded an averaged NIRAF ratio of 1.9 (95% Confidence interval: 1.8–2.1). Both the NIR imaging system and surgeon's visual confirmation yielded a 100% detection rate (9 out of 9 PGs).

Feasibility of enhancing PG visualization with OTIS is depicted in Fig. 6, *A*. As described earlier, the OTIS is regularly calibrated with a fluorescent ink grid (Fig. 6, *B*) to ensure that the visible projected image is aligned precisely (Fig. 6, *C*). Routine observation of operative field for a healthy PG (Fig. 6, *D*) without using the OTIS can be compared with enhanced visualization of the same gland using visible green light (Fig. 6, *E*) from the projection overlay of the OTIS. This is also demonstrated with similar precision for diseased PGs (Figs 6, *F* and 6, *G*). Averaged NIRAF ratio obtained with OTIS for healthy PGs ($n = 25$) was 5.2 (95% Confidence interval: 1.0–9.5), while that measured for diseased PGs ($n = 10$) was 6.8 (95% Confidence interval: 3.4–10.3). Overall, the OTIS successfully visualized 34 out of 35 PGs with a detection rate of 97%, whereas all PGs were accurately identified by the surgeon on visual examination. In 1 patient, a tissue suspected to be PG with low confidence by the surgeon was tested with OTIS and did not receive any visible projection overlay. This tissue was later histologically confirmed to be benign thyroid tissue indicating the specificity of OTIS.

All 3 optical modalities rely on detecting NIRAF of PGs in real time and do not require any contrast agent administration. Although all the 3 approaches demonstrate high and comparable PG detection rates when correlated with histologic validation (Table 2), the modified NIR imaging system and the OTIS pro-

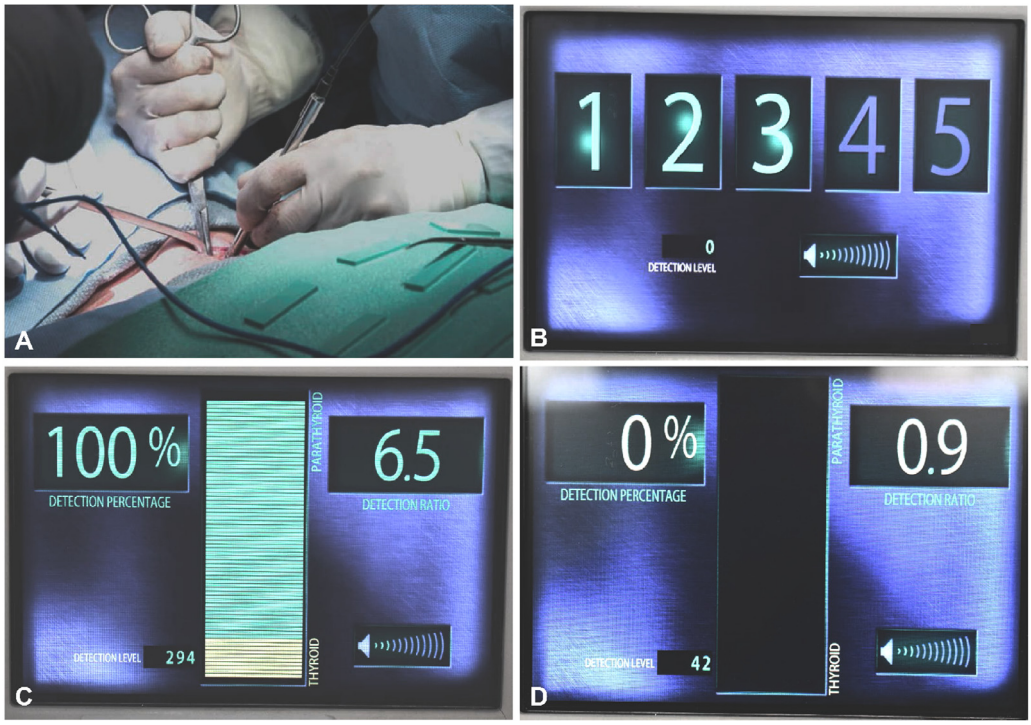

Fig. 4. (*A*) Handheld fiber-optic probe of the PTeye being placed onto tissue suspected to be parathyroid. (*B*) Thyroid near-infrared autofluorescence (NIRAF) baseline being established for the PTeye with measurements from 5 random spots on the thyroid. (*C*) Display interface when the tissue is identified as "positive" for parathyroid. (*D*) When the tissue is identified as "negative" for parathyroid. Detection ratio >1.2 was set as the threshold for parathyroid identification; the auditory feedback was kept inaudible and display interface was turned away from the surgeons during this study.

Table 2
Detection rates for the three NIRAF based optical modalities when correlated with histological validation.

	PTeye	(Modified) NIR imaging system	OTIS
Total number of participant surgeons	2	2	1
Tissues identified as parathyroid by visual examination (surgeon's degree of confidence)			
High	46 (83.6%)	9 (100.0%)	35 (97.2%)
Moderate	4 (7.3%)	0 (0.0%)	0 (0.0%)
Low	5 (9.1%)	0 (0.0%)	1 (2.8%)
Number of potential parathyroid glands seen	55	9	36‡
Number of parathyroid glands validated by histology	23	3	10
Accuracy			
Surgeon's detection rate for parathyroid glands (visually identified with high or moderate confidence)	50/55 (90.9%)	9/9 (100.0%)	35/35 (100.0%)
Device detection rate for parathyroid glands (glands left in-situ + excised glands validated by histology)	54/55 (98.2%)	9/9 (100.0%)	34/35 (97.1%)
Device detection rate for parathyroid glands (only excised glands validated by histology)	22/23 (95.6%)	3/3 (100.0%)	10/10 (100.0%)

‡ one specimen confirmed as benign thyroid tissue

vide additional spatial information regarding the PGs with the OTIS enabling direct PG visualization in the operative field. The PTeye scores higher than the other 2 modalities owing to its ability to identify PGs despite ambient OR lights that typically interfere with tissue NIRAF measurements. Quantitative comparison of the "detection ratio" (for PTeye) and NIRAF ratio (for the modified NIR imaging system and the OTIS) is represented in Fig. 7.

Discussion

Accurately identifying and then preserving PGs can prove challenging during neck operations because of distorted anatomy from previous interventions,[20] presence of ectopic or multiglandular diseased PGs,[7] extensive thyroid surgery with or without central neck lymph node dissection,[21] and varying experience or skillset of the surgeon.[8] In such scenarios, rapid and label-free intraoperative guidance to identify PGs would be beneficial for minimizing postoperative morbidity. Here, we showcase various innovative optical approaches that rely on NIRAF detection to provide surgical guidance for intraoperative PG identification. In our study, we evaluated and compared the performance of the PTeye—a device that utilizes a simple, handheld fiber-optic probe to guide PG identification, even in the presence of ambient OR lights; a modified version of a commercial NIR imaging system; and the OTIS—an imaging approach that projects visible images directly onto the operative field to enhance PG visualization.

Each system is endowed with a distinct set of features as summarized in Table 3. The main advantage of the PTeye is that it is a

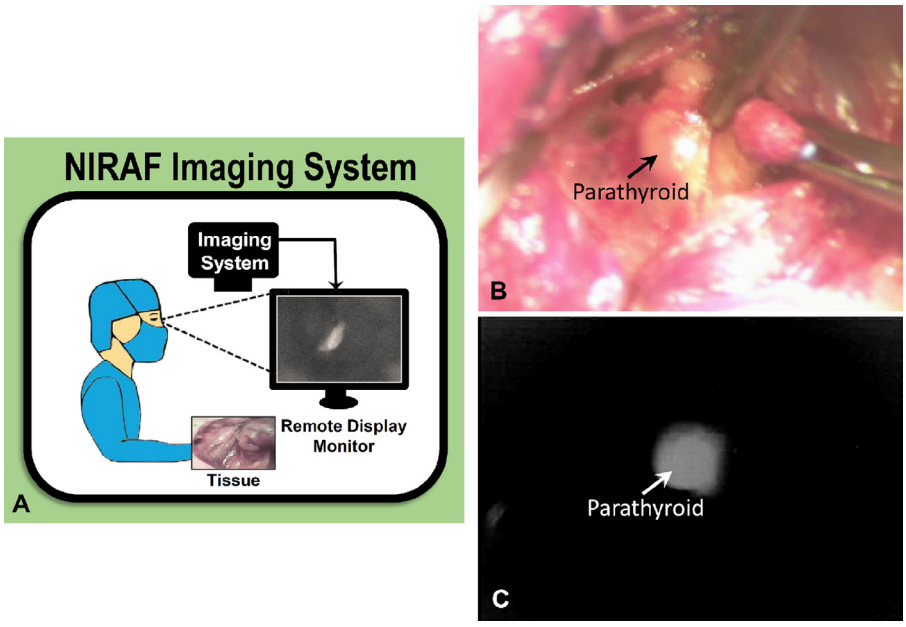

Fig. 5. (*A*) Intraoperative workflow when using the modified commercial near-infrared (NIR) imaging system. (*B*) White light image of the surgical field with a healthy parathyroid gland indicated by the *black arrow*. (*C*) Corresponding near-infrared autofluorescence (NIRAF) image showing the same parathyroid gland (denoted by the *white arrow*) with significantly higher NIRAF intensity compared to adjacent tissues in the background.
Note: The surgeons were blinded from the NIRAF images during this study.

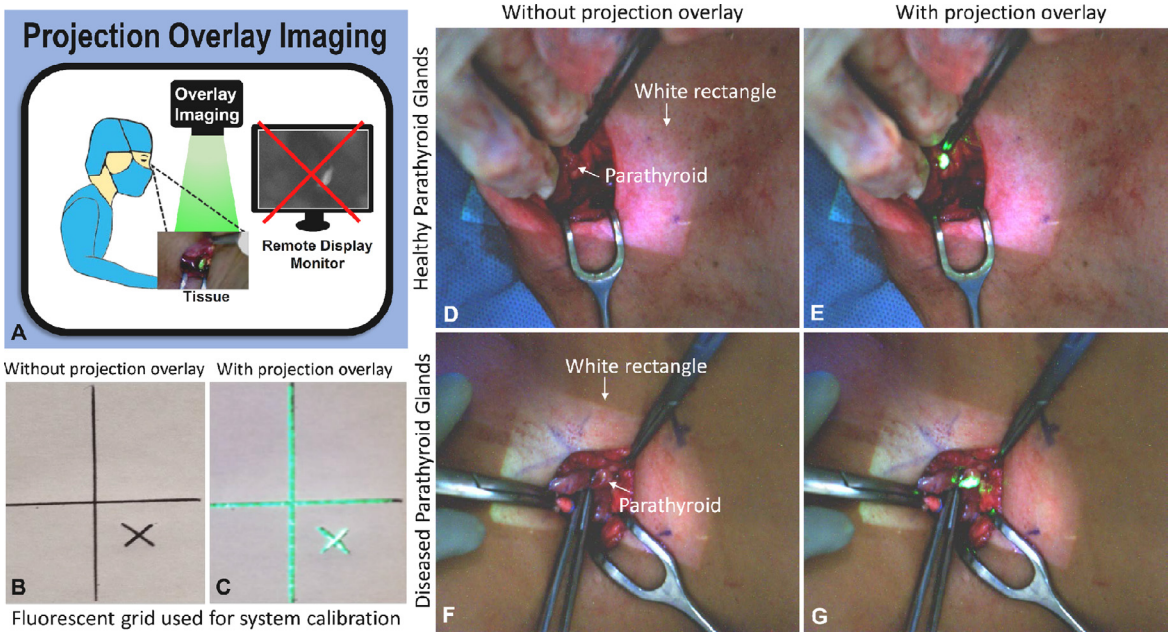

Fig. 6. (*A*) Intraoperative workflow while using the Overlay Tissue Imaging System (OTIS). (*B*) Grid sketched with near-infrared (NIR) fluorescent ink. (*C*) The OTIS calibration with the projected image overlay aligning precisely over the actual inked grid. (*D*) Surgical field without the projection overlay; *white arrow* denotes a healthy parathyroid gland as seen by the surgeon; the projected white rectangle aids in positioning the OTIS over the region of interest. (*E*) With the visible projection, the parathyroid is overlaid precisely with bright green light, with no overlay on the adjacent tissue structures. (*F*) Operative field without projection overlay and (*G*) with projection overlay for a diseased parathyroid gland.
Note: The surgeon looked away during the projection overlay.

compact device (33 cm × 22 cm × 15 cm) with a simple, handheld probe that aids in PG identification in the presence of OR lights, ensuring easy usage, portability, and storage. In contrast, the PTeye provides point-based measurements that do not provide spatial information of the structures surrounding the PGs that may be useful for the surgeon. Moreover, the PTeye has a contact-based approach mandating either sterilization of the fiber-optic probe for reusability in each new patient or using cost-effective disposable probes. These limitations are offset when utilizing the NIR imaging systems that can achieve wide-field imaging and provide spatial information of the PGs in relation to adjacent tissue structures. Although commercial NIR imaging systems can image a field of view of 900 cm^2,[22] our modified NIR imaging system covered a field of view measuring 5 cm × 5 cm (25 cm^2), which was ade-

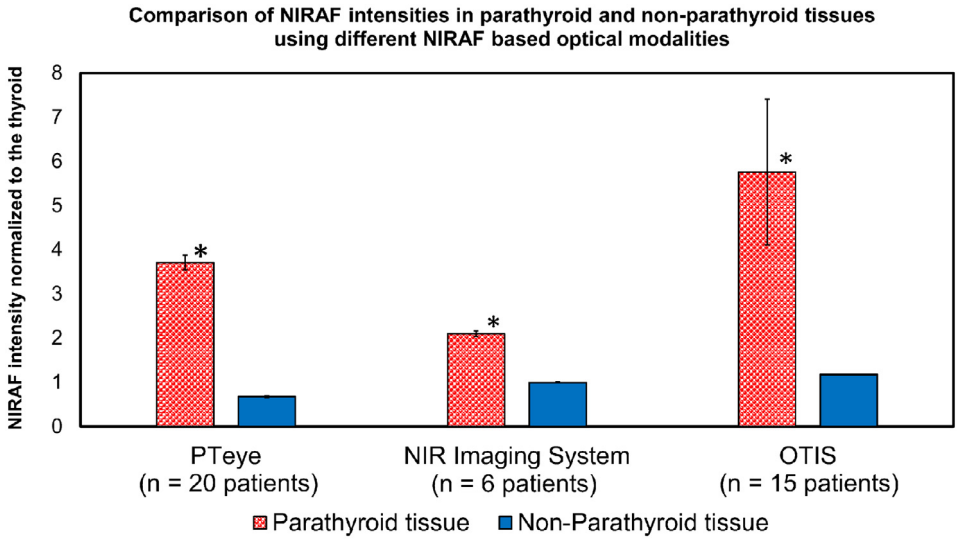

Fig. 7. Comparison of normalized near-infrared autofluorescence (NIRAF) intensities—detection ratio for the parathyroid eye (PTeye) and NIRAF ratio for the NIR imaging system and the Overlay Tissue Imaging System (OTIS)—for parathyroid and nonparathyroid tissues; parathyroid tissue exhibited greater normalized NIRAF intensities than nonparathyroid tissue consistently across all 3 optical modalities.
Error bar in figure represents standard error.
*P value $<$ .05.

quate considering that routine thyroid and parathyroid incisions range from 3–6 cm.[23] Although tissue contact is not required for this system, the NIR camera would still need to be covered with a sterile barrier material mainly because most commercial NIR cameras can capture images only at a working distance of 4–12 inches (10–30 cm) from the operative field,[22] which intrudes into the recommended sterile zone of 18 inches (50 cm) from the surgical plane.[24] Although NIRAF images are highly informative, grayscale images (as displayed in Fig. 5, *C*) may be interpreted incorrectly without adequate operative experience. In addition, having to stare at NIRAF images on a remote display monitor and correlate them with the real operative field could be tedious and distracting. The OTIS can circumvent this limitation by projecting NIRAF of PG as a visible image directly onto the operative field, thus providing true spatial context for the signal from PGs (Figs 6, *E* and 6, *G*). With the current system design, the OTIS can successfully function at a distance of 18 inches (50 cm) from the operative field and thus do not need to meet sterility requirements, unlike for the PTeye or the NIR imaging systems.

Ambient OR lights can prove problematic for NIRAF measurements with the NIR imaging system and the OTIS necessitating complete darkness in the OR, thus interrupting the surgical workflow. The applicability of these 2 optical modalities may also be limited when multiple PGs are present in a single field of view—a PG with greater NIRAF may obscure other PGs in an acquired image or when PGs are located at ectopic sites (tracheoesophageal groove or retro-esophageal region) that are not as easily visualized with imaging systems. In such scenarios, the PTeye is more convenient to use as the handheld probe can be easily positioned onto the target site for NIRAF measurements. The optimal functionality of the PTeye during tissue NIRAF measurements even in the presence of OR lights is an added advantage that is currently unmet by standard NIR imaging systems.

It should be emphasized that the PGs needed to be adequately dissected and exposed for evaluation with all 3 devices described in this study. This implies that NIRAF of PGs is more useful to confirm tissue identity only after the suspect tissue is first visualized by the surgeon. Because all 3 modalities employ NIR wavelengths that have limited tissue penetration depth (in mm), the potential to locate “missing” or deeply situated PGs is restricted, at least using the described approaches at present. Although some preliminary work of visualizing NIRAF of PGs below layers of fibrofatty tissue has been reported,[14] further investigations are needed to fully understand depth-based parathyroid NIRAF detection. Operative expertise still remains vital in correctly exposing, identifying, and subsequently preserving PGs in these scenarios.

The PG detection rate for the PTeye, the (modified) NIR imaging system and the OTIS stand at 98%, 100%, and 97%, respectively, suggesting that all 3 systems are viable operative guidance tools to aid in identifying PGs. Preference for either of the described NIRAF-based approaches would be governed by the surgeon’s choice, ease of use for the OR personnel, effortless integration to the existing workflow, availability, and cost of the device. Among the 3 systems, the learning curve for intraoperative implementation would be the shortest for the PTeye, as the instrument handling is very similar to nerve monitoring devices, such as Nerve Integrity Monitoring System (Medtronic, Dublin, Ireland) or Nerveana (Neurovision Medical Products, Ventura, CA), frequently used during thyroid operations[25] with which most surgeons are already familiar. Moreover, because this technique does not require OR lights to be switched off, the PTeye is relatively easier to use without disrupting surgical workflow compared with the other 2 modalities. Despite its inability to function with OR lights, using the NIR imaging system should not be complicated because surgeons have used similar modalities previously for visualization of tumor margins, sentinel lymph node mapping, lymphatic drainage, and blood flow visualization.[22] Notwithstanding the novel results provided by the OTIS, this system would have the longest learning curve of the 3 because the device is still in developmental stages and requires a user-friendly format before clinical use. Among the 3 modalities, NIR imaging systems are already commercially available worldwide,[22] some of which have already been investigated for intraoperative PG identification with high accuracy.[13–16] Most of these systems, however are not FDA-approved for label-free parathyroid NIRAF detection as of yet, while the PTeye was only FDA-approved for this application recently and is yet to become commercially available. In comparison, the OTIS needs to be optimized for a more simplistic user interface and operability inside the OR before commercialization. Although cost comparison between the 3 modalities is not presently feasible owing to the aforementioned factors, it must be

Table 3
Overview of the features and performance accuracy of the three NIRAF based optical modalities.

	PTeye	(Modified) NIR imaging system	OTIS
Features			
Data output	NIRAF detection intensity, detection ratio, device confidence in parathyroid identification (in %)	Grey scale NIRAF images on display monitor	NIRAF projected as visible image (in green color) onto surgical field
Functional component	Hand-held optical probe for point-based NIRAF detection	Portable NIR camera	Portable image projector
Spatial information	None	Yes	Yes
Working distance from surgical field	Contact based modality	15 cms	50 cms
Power fluence	20 mW over 600 μm spot size	1 W/cm^2	11.5 mW/cm^2
Spatial Resolution	N/A	170 μm	176 μm
Field of view per measurement	600 μm (point-based measurement)	5 cm × 5 cm	5 cm × 6.25 cm
Auditory feedback	Yes. (Inaudible during study)	No	No
Visual feedback	Device display	Remote display monitor	Direct projection onto surgical field
Sterility requirements	Sterilization for the detachable fiber-optic probe	Sterile barrier medium required for NIR camera	None. Disposable sterile handle attached for system positioning
Contrast agents	Not required	Not required	Not required
Ambient OR light interference	No	Yes	Yes
Commercial availability	No	Yes	No
Performance in patients	20 patients	6 patients	15 patients
Number of parathyroid glands assessed	55	9	35
Detection rate	98.2% (54/55 parathyroids)	100% (9/9 parathyroids)	97.1% (34/35 parathyroids)
Healthy parathyroid glands	100% (33/33 parathyroids)	100% (6/6 parathyroids)	96.0% (24/25 parathyroids)
Diseased parathyroid glands	95.5% (21/22 parathyroids)	100% (3/3 parathyroids)	100% (10/10 parathyroids)
Sensitivity	97.2% (104/107)*	N/A†	97.1 (34/35)
Specificity	94.9% (188/198)	N/A†	100% (1/1)‡
Overall accuracy	95.7%	N/A†	97.2%
Advantages	(i) Compact and portable unit (ii) Hand-held point-based guidance technique (iii) Intuitive user-interface (iv) Functional with OR lights	(i) Wide field imaging technique (ii) Spatial information of parathyroid acquired (iii) Commercial devices available	(i) Spatial information of parathyroid acquired (ii) Enhanced visualization directly in surgical field (iii) No display interface or monitors required
Disadvantages	(i) No spatial information provided. (ii) Not commercially available as yet	(i) Affected by OR lights (ii) Interpretative errors due to mismatch between NIRAF image and surgical field of view	(i) Affected by OR lights (ii) User-interface requires further simplification (iii) Not commercially available as yet

* Measurement on 1-2 sites in all parathyroid glands
† NIR imaging performed only for parathyroid glands and not for thyroid, fat, muscle
‡ single non-parathyroid tissue tested - thyroid

noted that purchasing either of the 3 systems is eventually a one-time investment for the hospital followed by periodic maintenance costs to ensure optimal performance when compared with recurrent costs incurred per frozen section analysis and prolonged duration of anesthesia maintenance for each patient.

Despite the various innovations for intraoperative PG identification elaborated in this study, these optical tools may only serve as adjuncts to the experience, skill set, and knowledge of the surgeon. Experienced endocrine surgeons can correctly identify PGs without major challenges by simply relying on visual examination and their experience. Data analysis indicates that our participant surgeons accurately identified PGs with high/moderate confidence by visual confirmation in 91% of the PGs assessed with the PTeye and 100% for those tested with the NIR imaging system and the OTIS (overall surgeon accuracy: 95%). NIRAF detection modalities for PGs may, therefore, stand to be more beneficial for early career or low-volume-center surgeons who tend to have greater complication rates.[8] In procedures with extensive thyroid and associated lymph node dissection, even highly experienced surgeons face the possibility of incidental damage to the PGs or its vasculature, which can be minimized by detecting NIRAF of PGs. This approach can then aid in decision-making to autotransplant an accidentally excised PG. Although these NIRAF-based modalities may not differentiate between healthy and diseased PGs, these techniques can still be valuable during parathyroidectomies because surgeons are occasionally challenged in distinguishing between a diseased PG and other tissues, such as a benign thyroid nodule or an enlarged lymph node. Nonetheless, for parathyroidectomies, these NIRAF-based modalities work best as adjunct tools along with the existing protocol of intraoperative parathyroid hormone monitoring. Another prime advantage gained with these real-time devices would be a decrease in the time and expense associated with each unnecessary frozen biopsy sent for PG confirmation. A recent study demonstrated that NIRAF-based PG detection could potentially improve patient outcomes by minimizing the incidence of postsurgical hypocalcemia after thyroid operations.[16] Innovative optical modalities developed for NIRAF detection in PGs could thus be used for label-free surgical guidance to conserve healthy PGs during thyroid operations or aid in removing diseased PGs through parathyroidectomies for decreasing postoperative complications and needless costs.

Acknowledgments

We would like to thank the OR staff for their assistance in data collection. This study was supported by the National Institutes of Health under grant no. 1R01CA212147-01A1, R42CA192243 and the National Science Foundation Graduate Research Fellowship Program under grant no. 0909667.

Conflicts of interest

Professor Anita Mahadevan-Jansen and Vanderbilt University have a licensing agreement with AIBiomed Instruments (Santa Barbara, CA) for developing the PTeye. AIBiomed Instruments is the exclusive licensee of the intellectual property on the NIRAF detection technique from Vanderbilt University. The authors indicate that they have no other conflicts of interest regarding the content of this article.

References

1. Applewhite MK, White MG, Xiong M, Pasternak JD, Abdulrasool L, Ogawa L, et al. Incidence, risk factors, and clinical outcomes of incidental parathyroidectomy during thyroid surgery. *Ann Surg Oncol*. 2016;23:4310–4315.
2. Tang JA, Salapatas AM, Bonzelaar LB, Friedman M. Parathyroidectomy for the treatment of hyperparathyroidism: thirty-day morbidity and mortality. *Laryngoscope*. 2018;128:528–533.
3. Simental A, Ferris RL. Reoperative parathyroidectomy. *Otolaryngol Clin North Am*. 2008;41:1269–1274.
4. Wachtel H, Cerullo I, Bartlett EK, Kelz RR, Karakousis GC, Fraker DL. What can we learn from intraoperative parathyroid hormone levels that do not drop appropriately. *Ann Surg Oncol*. 2015;22:1781–1788.
5. Doherty GM, Weber B, Norton JA. Cost of unsuccessful surgery for primary hyperparathyroidism. *Surgery*. 1994;116:954–958.
6. Mohebati A, Shaha AR. Imaging techniques in parathyroid surgery for primary hyperparathyroidism. *Am J Otolaryngol*. 2012;33:457–468.
7. Chen H, Wang TS, Yen TWF, Doffek K, Krzywda E, Schaefer S, et al. Operative failures after parathyroidectomy for hyperparathyroidism: the influence of surgical volume. *Ann Surg*. 2010;252:691–695.
8. Sosa JA, Bowman HM, Tielsch JM, Powe NR, Gordon TA, Udelsman R. The importance of surgeon experience for clinical and economic outcomes from thyroidectomy. *Ann Surg*. 1998;228:320–330.
9. Novis DA, Zarbo RJ. Interinstitutional comparison of frozen section turnaround time. *Arch Pathol Lab Med*. 1997;121:559.
10. Ahuja AT, Wong KT, Ching ASC, Fung MK, Lau JYW, Yuen EHY, et al. Imaging for primary hyperparathyroidism—what beginners should know. *Clinical Radiology*. 2004;59:967–976.
11. Paras C, Keller M, Mahadevan-Jansen A, White L, Phay J. Near-infrared autofluorescence for the detection of parathyroid glands. *BIOMEDO*. 2011;16.
12. McWade MA, Sanders ME, Broome JT, Solórzano CC, Mahadevan-Jansen A. Establishing the clinical utility of autofluorescence spectroscopy for parathyroid detection. *Surgery*. 2016;159:193–203.
13. De Leeuw F, Breuskin I, Abbaci M, Casiraghi O, Mirghani H, Ben Lakhdar A, et al. Intraoperative near-infrared imaging for parathyroid gland identification by auto-fluorescence: a feasibility study. *World J Surg*. 2016;40:2131–2138.
14. Kim SW, Song SH, Lee HS, Noh WJ, Oak C, Ahn Y-C, et al. Intraoperative real–time localization of normal parathyroid glands with autofluorescence imaging. *J Clin Endocrinol Metab*. 2016;101:4646–4652.
15. Falco J, Dip F, Quadri P, de la Fuente M, Prunello M, Rosenthal RJ. Increased identification of parathyroid glands using near infrared light during thyroid and parathyroid surgery. *Surg Endosc*. 2017;31:3737–3742.
16. Benmiloud F, Rebaudet S, Varoquaux A, Penaranda G, Bannier M, Denizot A. Impact of autofluorescence-based identification of parathyroids during total thyroidectomy on postoperative hypocalcemia: a before and after controlled study. *Surgery*. 2018;163:23–30.
17. Berguer R. Surgery and ergonomics. *Archives of surgery*. 1999;134:1011–1016.
18. Elliott JT, Dsouza AV, Davis SC, Olson JD, Paulsen KD, Roberts DW, et al. Review of fluorescence guided surgery visualization and overlay techniques. *Biomed Opt Express*. 2015;6:3765–3782.
19. McWade MA, Paras C, White LM, Phay JE, Solorzano CC, Broome JT, et al. Label-free intraoperative parathyroid localization with near-infrared autofluorescence imaging. *The* J Clin Endocrinol Metab. 2014;99:4574–4580.
20. Lin DT, Patel SG, Shaha AR, Singh B, Shah JP. Incidence of inadvertent parathyroid removal during thyroidectomy. *The Laryngoscope*. 2002;112:608–611.
21. Bergamaschi R, Becouarn G, Ronceray J, Arnaud J-P. *Am J Surgery*. 1998;176:71–75.
22. Zhu B, Sevick-Muraca E. A review of performance of near-infrared fluorescence imaging devices used in clinical studies. *British J Radiol*. 2014;88.
23. Brunaud L, Zarnegar R, Wada N, Ituarte P, Clark OH, Duh Q. Incision length for standard thyroidectomy and parathyroidectomy: when is it minimally invasive. *Archives of Surgery*. 2003;138:1140–1143.
24. Price P, Frey KB. *Microbiology for surgical technologists*. Boston, Massachusetts, USA: Cengage Learning; 2003:85–96.
25. Angelos P. Recurrent laryngeal nerve monitoring: state of the art, ethical and legal issues. *Surgical Clinics*. 2009;89:1157–1169.

Discussion

Dr Michael Campbell (Sacramento, CA): Great study. I have been looking into this technology and the more I learn about it, the more I realize how excellent the work coming out of Vanderbilt really is. I want to congratulate your whole team on that.

Specifically, with the PTeye, you are really relying on the surgeon having an inclination that something is a parathyroid and then confirming it. When you are talking about helping low-volume surgeons, it becomes somewhat difficult because they might have seen 1 or 2 parathyroids a year, and they don't really know if it's fat or parathyroid tissue.

Is there any way to move the PTeye to the next step beyond doing point measurements to doing scans? In other words, being able to look over a larger field to help them say, "Okay, this area looks like there's a parathyroid here, this looks like fat, this looks like thyroid"?

Dr Giju Thomas: That's essentially what the second modality does with the near-infrared imaging camera, which gives you a field of view of roughly 5 centimeters by 5 centimeters. With that, the parathyroid would glow while something like fat or thyroid, wouldn't glow. The idea is to provide a surgeon what he or she prefers in the end. So if you are looking for a scanner, the best modality to go for would be a near-infrared imaging camera because you get to see an entire field of view.

Dr John Phay (Columbus, OH): Giju, very nice job and well-presented. The pictures of the overlay were spectacular.

Is the penetrance of detection different between the modalities? Does the PTeye have any better, deeper penetrance in terms of the thickness of the tissue as compared to the other options?

Dr Giju Thomas: Thank you for that wonderful question, Dr Phay. One thing we must realize is that deeper tissue penetration with near infrared light would depend on interplay between certain factors like laser power used and the optical property of the tissue that overlies the parathyroid gland. With the probe, you have the advantage that it is directly in contact with the tissues. So the chances of the near-infrared going deeper is much higher. But with near-infrared imaging systems and OTIS, the idea is that you may need to crank up the power to a point. But near-infrared light can go only as deep as maybe a few millimeters at the most. So that is always going to be a limitation.

The other aspect as I mentioned earlier is the optical property of the tissue that lies above the parathyroid. There was a previous study documenting that the authors were able to see parathyroid glands below a certain layer of fat, but they didn't specify how thick or thin the layer of fat was. You could potentially detect parathyroid glands under about 2 or 3 millimeters of fat, but you wouldn't find something like an intrathyroidal parathyroid, which

is buried deep within the thyroid gland. This is because thyroid tissue has different optical properties compared to fat.

Dr John Phay (Columbus, OH): One other question. As you know, most fluorescence-guided surgery is based on indocyanine green, which admittedly is similar but not exactly the same. Do you know if the overlay system would work for ICG imaging?

Dr Giju Thomas: Yes. Even though we have patented this particular form of projection overlay for parathyroid visualization, fluorescence overlay projection for contrast agents like ICG has been investigated in earlier studies for applications such as tumor margin guidance and sentinel lymph node mapping.

Dr Quan-Yang Duh (San Francisco, CA): This is really exciting. We tried some of these techniques, and I believe that 5 years from now we will be hearing papers here very similar to the neuromonitoring experience. There will be arguments about whether or not you save parathyroids. My bet is that we will not be, but we will still be using it just like neuromonitoring.

The question I have for you is in terms of which one is better, et cetera. It will most likely come down to how much it costs. So what is the anticipated per-case cost for the different modalities?

Dr Giju Thomas: A fine question for a biomedical engineer.

Let me give the facts here. To build a device like the PTeye in the lab didn't cost much. It cost $5,000 to $8,000 just to build a system like that. When you partner with a company and commercialize it, what they tend to do is add a factor of 2 or 3 to make it profitable. So I can't give a definite number for how much the PTeye is going to cost in clinical use.

On the other hand, you have the near-infrared imaging cameras. I found out that the Hamamatsu system costs roughly around $80,000. These NIR cameras are not exclusively used for parathyroid identification and have multiple applications which also includes ICG-based contrast.

So on one side you have a larger device that would cost more but can be used for multiple purposes. And on the other side, you have a relatively simple, compact and economical device like PTeye which is specifically designed for parathyroid identification as the name implies. The choice of investing in either devices would be dictated by a surgeon's preference and the volume of thyroid/parathyroid surgeries happening at the respective medical centers.

Dr Cortney Lee (Lexington, KY): Regarding the depth of penetration, it would be nice if it could help you find the parathyroid to begin with, but I know it's limited. Most patients have more than a few millimeters of fat covering things. But from a practical standpoint with the PTeye and the point probe, it seems like you will still cut down on time for frozen section.

Dr Giju Thomas: At the moment, you are cutting down the time as well as the cost. Surgeons typically tend to wait for the frozen section results before taking the next surgical step. Until recently, I did not realize that when a surgeon waited extra 20–30 minutes for surgical pathology results, that it added further onto anesthesia and OR costs, in addition to expenses associated with frozen section analysis itself. In that sense it could be very beneficial for not just minimizing the wait-time for surgeons, but also in terms of cutting costs borne by patients as well.